PAPER

$Mo_{0.5}W_{0.5}S_2$ for Q-switched pulse generation in ytterbium-doped fiber laser

To cite this article: Junli Wang *et al* 2018 *Nanotechnology* **29** 224002

IOP Publishing Nanotechnology
Nanotechnology 29 (2018) 224002 (7pp) https://doi.org/10.1088/1361-6528/aab5f2

$Mo_{0.5}W_{0.5}S_2$ for Q-switched pulse generation in ytterbium-doped fiber laser

Junli Wang[1], Lei Chen[1], Chenxi Dou[1], Haiting Yan[2], Lingjie Meng[2] and Zhiyi Wei[3]

[1] School of Physics and Optoelectronic Engineering, Xidian University, Xi'an, People's Republic of China
[2] School of science, Xi'an Jiao Tong University, Xi'an, People's Republic of China
[3] Beijing Nation Laboratory for Condensed Matter Physics, Institute of Physics, Chinese Academy of Sciences, Beijing, People's Republic of China

E-mail: dispersion@126.com

Received 15 January 2018, revised 2 March 2018
Accepted for publication 12 March 2018
Published 4 April 2018

Abstract

In this work, we fabricate the $Mo_{0.5}W_{0.5}S_2$ by microwave-assisted solvothermal method, and report the Q-switched Yb-doped fiber lasers (YDFL) using $Mo_{0.5}W_{0.5}S_2$ polymer film and tapered fiber as the saturable absorbers (SAs). The modulation depth and saturable intensity of the film SA are 5.63% and 6.82 MW cm^{-2}. The shortest pulse duration and the maximum single pulse energy are 1.22 μs and 148.8 nJ for the film SA, 1.46 μs and 339 nJ for the fiber-taper SA. To the best of our knowledge, this is the first report on the Q-switched YDFL using $Mo_{0.5}W_{0.5}S_2$ SAs.

Keywords: Q-switched lasers, fiber lasers, nanomaterials, ultrafast nonlinear optics

(Some figures may appear in colour only in the online journal)

1. Introduction

Passively Q-switched fiber lasers have been widely investigated owing to their potential applications in optical communications, remote sensing, medicine, and material process [1–3]. Unlike the mode-locked fiber lasers which generally exhibit wide optical spectrum and ultrashort pulses, the Q-switched fiber lasers typically generate microsecond or nanosecond pulses with high pulse energy. Besides, Passively Q-switched fiber lasers are attractive due to their cost, efficient operation, and easy implantation without much considering of dispersion and nonlinearity [4]. In recent years, a wide variety of SAs have been used in fiber lasers to obtain Q-switched laser pulses. Semiconductor saturable absorber mirrors (SESAMs), single-wall carbon nanotubes (SWCNTs) have been extensively studied and demonstrated in passively Q-switched fiber lasers [5, 6]. SESAMs are mature SAs for their flexibility and robustness. However, the narrow operating bandwidth and high fabrication cost limit their application. For SWCNTs, the absorption wavelength is depend on the nanotube diameter, which means that they are not efficient. The emergence of two-dimensional (2D) materials effectively solve the problems above.

The discovery of graphene has given birth to the 2D materials. New 2D materials, such as topological insulator, transition metal dichalcogenides (TMDs) and black phosphorus have been reported to possess unique optoelectronic properties and Pauli blocking induced saturable absorption [7–14]. Among these excellent 2D materials, TMDs have attracted much research interest. The typical chemical structure of TMDs is MX_2, the transition metal (M) atoms (M: such as Mo, W) are covalently bound to the chalcogen (X) atoms (X: such as S, Se) and the MX_2 layers are stacked together by van der Waals forces. They have a layer-dependent bandgap and can transition from indirect bandgap (bulk states) to direct band gap (monolayer or few layers) by reducing the number of layers. TMDs including molybdenum disulphide (MoS_2), molybdenum diselenide ($MoSe_2$), tungsten disulphide (WS_2), and tungsten diselenide (WSe_2) have demonstrated that they are ideal SAs for Q-switching fiber lasers [15–18]. The successful application of TMDs on Q-switched fiber lasers has brought great motivation to develop new types of TMDs materials.

Band gap engineering of monolayer 2D materials is of great significance on the optoelectronics applications [19, 20]. Combining of materials with different bandgap into alloy

could effectively modify their bandgaps [21]. Xie *et al* have extensively studied the preparation, characterization and application of 2D TMDs alloys [22, 23]. Mixed molybdenum tungsten disulphide ($Mo_{1-x}W_xS_2$) is a new type of the TMDs. Chen *et al* demonstrate that the bandgap emission of 2D alloys ($Mo_{1-x}W_xS_2$ monolayers) could be tuned from 1.82 to 1.99 eV [24]. The bandgap tunable property may enhance the broadband saturable absorptive capacity of the TMDs materials. However, the study of the nonlinear optical properties of $Mo_{1-x}W_xS_2$ is insufficient, whereas the application on the Q-switched fiber lasers has not been reported yet. The Z-scan measurements of $Mo_{0.5}W_{0.5}S_2$ at 1064 nm indicated that multilayer $Mo_{0.5}W_{0.5}S_2$ has a large two-photon absorption (TPA) coefficient and exhibits reverse saturable absorption under high excitation intensity [25]. In this case, $Mo_{0.5}W_{0.5}S_2$ may has potential application on Q-switching lasers.

In this work, we demonstrate the Q-switching operation in Yb-doped fiber lasers (YDFL) based on $Mo_{0.5}W_{0.5}S_2$ SAs. The $Mo_{0.5}W_{0.5}S_2$ is fabricated by microwave-assisted solvothermal method (MAST) [26] and its polymer film is inserted into the fiber cavity. Gradually increasing the pump power, stable Q-switched pulses are obtained. The maximum output power and pulse energy are 13.26 mW and 148.8 nJ for the film SA. The fiber-taper $Mo_{0.5}W_{0.5}S_2$ SA is also prepared by optical driven deposition method in this work. The small waist diameter (4 μm) of the tapered fiber enables a strong interaction between laser pulses and the $Mo_{0.5}W_{0.5}S_2$ SA. The maximum pulse energy of 339 nJ and the minimum pulse duration of 1.46 μs are obtained based on the fiber-taper $Mo_{0.5}W_{0.5}S_2$.

2. Preparation and characterization of $Mo_{0.5}W_{0.5}S_2$ SAs

Film saturable absorber (SA) is widely used in the Q-switched fiber lasers for their uniform quality and flexibility to integrate into the laser cavities. The $Mo_{0.5}W_{0.5}S_2$ embedded in Polyvinyl Alcohol (PVA) film is prepared in the work. Firstly, 4 g PVA powder is added into 100 ml deionized water and the mixture is stirred at 50 °C for 30 min. When the PVA is completely dissolved, 5 mg $Mo_{0.5}W_{0.5}S_2$ powder is added into 60 ml PVA solution. After stirring and ultra-sonicating for 2 h, the $Mo_{0.5}W_{0.5}S_2$ is uniformly dispersed in the PVA solution. Then the mixture is dropping onto a culture dish and evaporating in a vacuum drying oven for 12 h. When the $Mo_{0.5}W_{0.5}S_2$ PVA solution is completely dry, a transparent polymer film can be obtained. The $Mo_{0.5}W_{0.5}S_2$ nanosheets are embedded in the polymer film. Finally, the transparent polymer film is cut into small pieces of $1 \times 1\,mm^2$ and sandwiched between two fiber patch cords, as shown in figure 1(a). The function of the fiber patch cord is to connect two optical fibers together and the optical fiber core is entirely covered by the PVA film. The laser directly transmits the $Mo_{0.5}W_{0.5}S_2$-PVA film, enabling a strong interaction between the SA and the laser pulses.

An alternative approach to prepare SAs is applied by depositing the 2D materials to the tapered fiber surface. In this

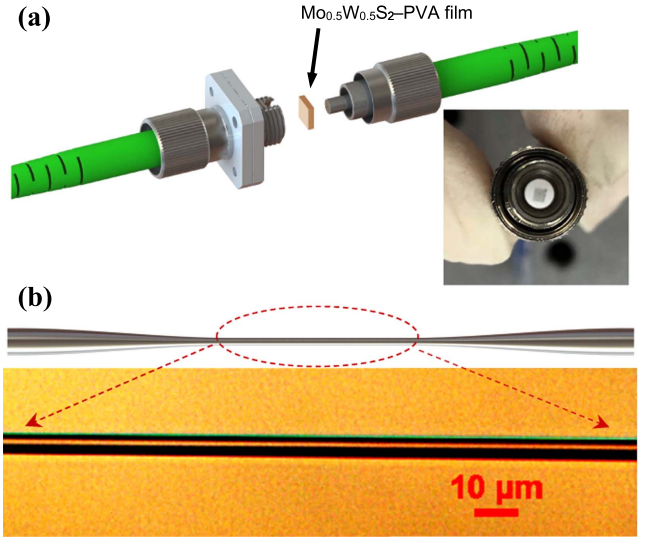

Figure 1. (a) Schematic showing integration of $Mo_{0.5}W_{0.5}S_2$ SA device between two fiber patch cords, the inset shows the facet of a fiber patch cord covered with $Mo_{0.5}W_{0.5}S_2$-PVA film. (b) Schematic of the tapered fiber (above) and the microscopic image (below) of the taper region.

case, the 2D material is not directly interacted with the laser pulses but with the evanescence wave. This type of SAs takes the advantage of high thermal damage threshold and long interacting length [27]. Therefore, we deposit the $Mo_{0.5}W_{0.5}S_2$ nanosheets onto the tapered fiber. The $Mo_{0.5}W_{0.5}S_2$ nanosheets solution is obtained by dissolving 25 mg $Mo_{0.5}W_{0.5}S_2$ powder in 20 ml ethanol solvent with 3 h ultra-sonicating. The tapered fiber we used in our experiment has a taper length of 21 mm. Figure 1(b) shows the image of the tapered fiber, the microscopic image of the tapered region indicates that the waist diameter is about 4 μm. The tapered fiber is then transferred into a U-slot and packaged in a silica tube. We drop the $Mo_{0.5}W_{0.5}S_2$ nanosheets solution onto the tapered fiber surface and insert it into the laser cavity for optical driven deposition.

The transmission electron microscope image of $Mo_{0.5}W_{0.5}S_2$ nanosheets is shown in figure 2(a). High quality few layer nanosheets can be observed at the edge of the cluster. Figure 2(b) is the EDX spectra from the selected section of the SEM image and the analysis results in the table 1 for the $Mo_{0.5}W_{0.5}S_2$ sample. The sample contains S, Mo and W elements, the atomic ratio of which is 62.27:18.08:19.65. We characterize and compare the WS_2, $Mo_{0.5}W_{0.5}S_2$, and MoS_2 with the x-ray diffraction method. In figure 2(c), the diffraction peaks of the $Mo_{1-x}W_xS_2$ ($x = 1$, 0.5, 0) alloy have three broad peaks at around $2\theta = 14.7°$, 33.1° and 58.8° corresponding respectively to the (002), (100), and (110) planes of the hexagonal $Mo_{1-x}W_xS_2$, which indicates the deficient crystalline in the sample. This is ascribed to the limitation of the MAST method and the W, Mo atom difference in the $Mo_{0.5}W_{0.5}S_2$ sample.

To further verify the nonlinear optical properties of $Mo_{0.5}W_{0.5}S_2$-PVA, we built a twin-detector measurement system. A homemade ultrafast YDFL is used as the illumination light. The repetition rate, center-wavelength and the

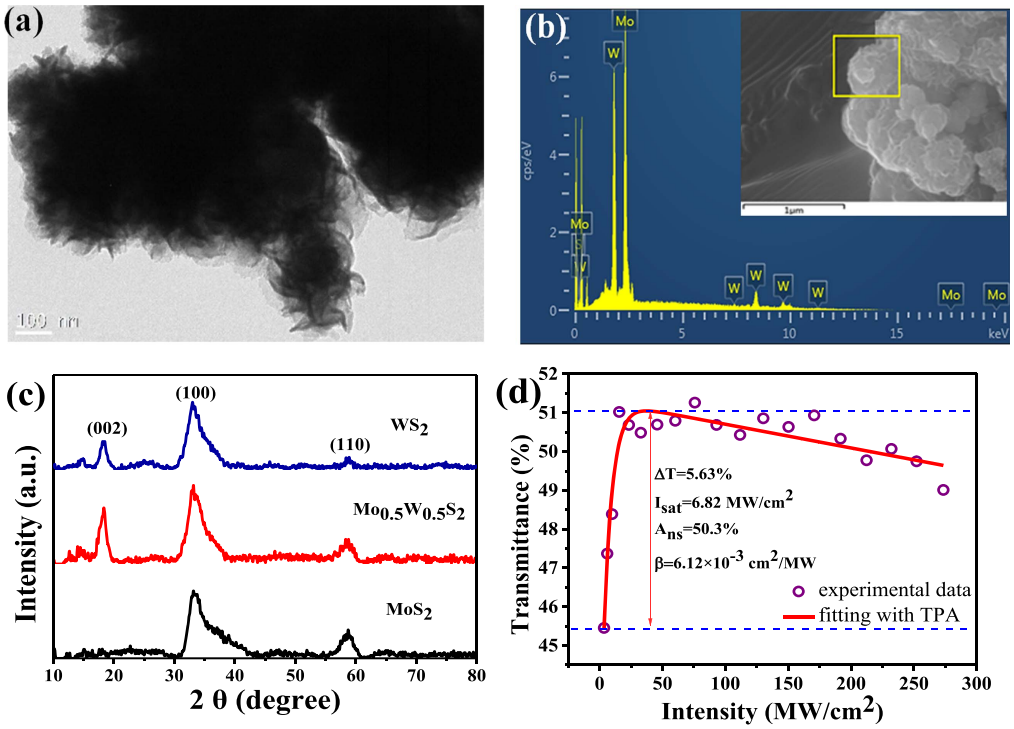

Figure 2. (a) Transmission electron microscope of the $Mo_{0.5}W_{0.5}S_2$ nanosheets. (b) Energy Dispersive x-ray spectroscopy of the $Mo_{0.5}W_{0.5}S_2$ nanosheet, the inset shows the SEM image of the selected section. (c) X-ray diffraction image of the WS_2, $Mo_{0.5}W_{0.5}S_2$ and the MoS_2. (d) Nonlinear saturable absorption of the $Mo_{0.5}W_{0.5}S_2$-PVA film.

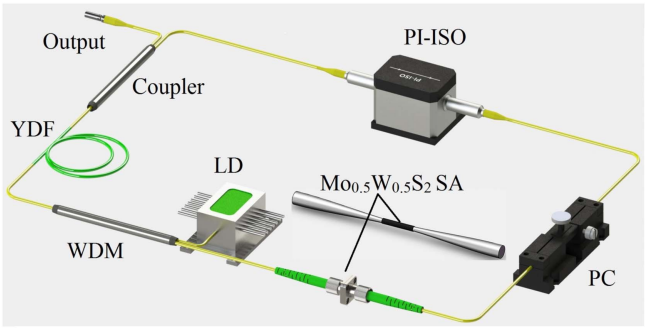

Figure 3. Schematic of the all-fiber Q-switched YDF laser cavity. LD: laser diode; WDM: wavelength division multiplexer; YDF: Ytterbium-doped fiber; PI-ISO: polarization independent isolator; PC: polarization controller; $Mo_{0.5}W_{0.5}S_2$ SA: fiber-taper $Mo_{0.5}W_{0.5}S_2$ SA and $Mo_{0.5}W_{0.5}S_2$-PVA film SA (the film SA is sandwiched between two fiber connectors).

Table 1. Elemental analysis of $Mo_{0.5}W_{0.5}S_2$ sample.

Element	Line	k-ratio	Weight%	Wt% sigma	Atomic%
S	K-lines	0.206 22	27.19	1.17	62.27
Mo	L-lines	0.16 020	23.62	2.31	18.08
W	M-lines	0.42 499	49.19	1.67	19.65
Total			100.00		100.00

duration of the pulses are 39.38 MHz, 1030 nm, 3.7 ps respectively. The previous report about multilayer $Mo_{0.5}W_{0.5}S_2$ indicated that this material processes a large TPA coefficient [25]. The transmittance of the SA decreased at high input intensity. In this case, we fit the data with the formula [28]:

$$T(I) = 1 - \Delta T \times \exp(-I/I_{sat}) - A_{ns} - \beta I.$$

Where T is the transmittance, ΔT is the modulation depth, I is the intensity of laser, I_{sat} is the saturation intensity, A_{ns} is the non-saturable absorbance and β is the TPA coefficient. Figure 2(d) shows the nonlinear saturable absorption of the $Mo_{0.5}W_{0.5}S_2$ SA. The $Mo_{0.5}W_{0.5}S_2$-PVA film has a modulation depth of 5.63% corresponding to the saturation intensity of 6.82 MW cm^{-2}. The non-saturable absorbance is 50.3% and the TPA coefficient is about 6.12×10^{-3} cm^2 MW^{-1}.

3. Results and discussion

The schematic of the all-fiber Q-switched YDFL based on $Mo_{0.5}W_{0.5}S_2$ SAs is shown in figure 3. Gain media with Ytterbium-doped fiber (YDF) is capable of emiting laser in 1 μm wavelength range and there are many attractive researches on the application of YDF [29–32]. The gain medium used in our experiment is a 25 cm YDF with high absorption coefficient (1200 dB m^{-1} at 976 nm). The YDF is pumped by a tunable laser diode with 976 nm center wavelength and 700 mW maximum output power. The pump laser is coupled into the YDF by a 976/1030 nm wavelength division multiplexer. A polarization independent isolator is used to prevent the bidirectional transmission in the laser cavity. A polarization controller (PC) is used to adjust the polarization state of laser in the cavity. A 40/60 coupler is

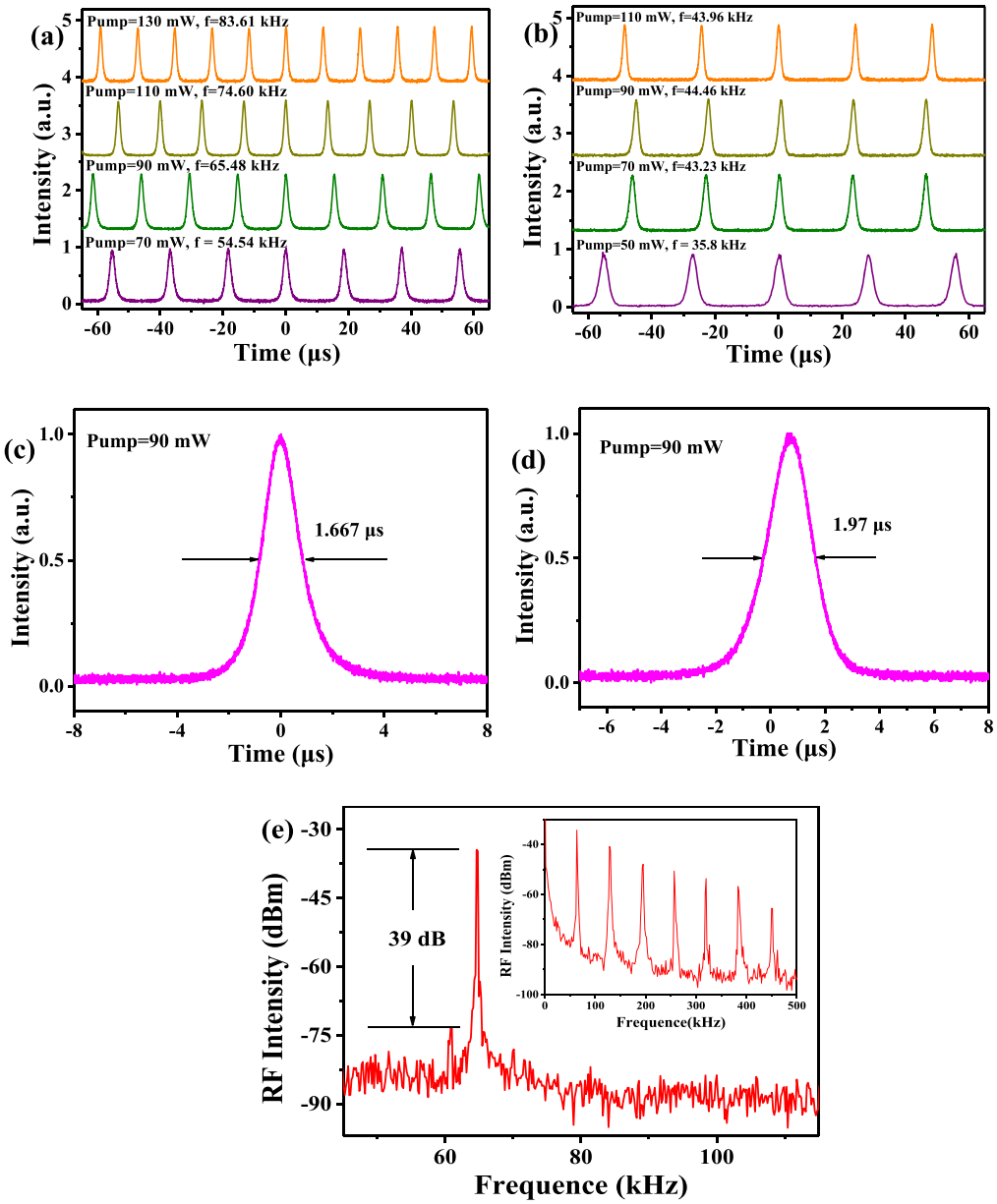

Figure 4. Q-switched Pulse train at different pump power and pulse width at 90 mW pump power based on (a), (c) $Mo_{0.5}W_{0.5}S_2$-PVA film SA and (b), (d) Fiber-taper $Mo_{0.5}W_{0.5}S_2$ SA. (e) RF spectra (measured with 100 Hz RBW) of Q-switching operation with $Mo_{0.5}W_{0.5}S_2$ film SA at the pump power of 90 mW.

used to output the laser emission for further using or monitoring. An Optical Spectrum Analyzer (Ocean optics HR2000 + CG) and an oscilloscope (Tektronix DOP 3052) with high speed photodetector are used to monitor the output spectrum and the pulse trains. The $Mo_{0.5}W_{0.5}S_2$-PVA film is cut into small pieces of 1 × 1 mm^2 and sandwiched between two fiber connectors. The setup for the fiber-taper $Mo_{0.5}W_{0.5}S_2$ SA is consistent with the former. We just replaced the fiber connectors with a tapered fiber.

The Q-switching operations of fiber laser based on $Mo_{0.5}W_{0.5}S_2$-PVA film SA and fiber-taper $Mo_{0.5}W_{0.5}S_2$ SA are quite different. Continues wave operation are observed for both the film SA and the fiber-taper SA when the pump power up to 30 mW. Through increasing the pump power and carefully adjusting the PC, Q-switched pulses are generated at 50 mW and 40 mW, respectively. Figures 4(a) and (b) shows the typically Q-switched pulse train of the $Mo_{0.5}W_{0.5}S_2$-PVA film SA and fiber-taper $Mo_{0.5}W_{0.5}S_2$ SA. In figure 4(a), When the pump power is set at 70, 90, 110 and 130 mW, stable Q-switched pulse train are obtained, the repetition rate are 54.54, 65.48, 74.60 and 83.61 kHz. For the Q-switched pulse with fiber-taper $Mo_{0.5}W_{0.5}S_2$ SA, as shown in figure 4(b), the repetition rate are 35.8, 43.23, 44.46 and 43.96 kHz, corresponding to the pump power of 50, 70, 90 and 110 mW. The symmetrical Gaussian-shaped pulses in figures 4(c) and (d) show the pulse width of 1.667 and 1.97 μs for the film SA and fiber-taper SA at 90 mW. The oscilloscope traces without pulse modulation in figures 4(a) and (b) also indicate the Q-switching operation are stable. We measured the radio frequency (RF) output spectrum of the pulse trains as shown

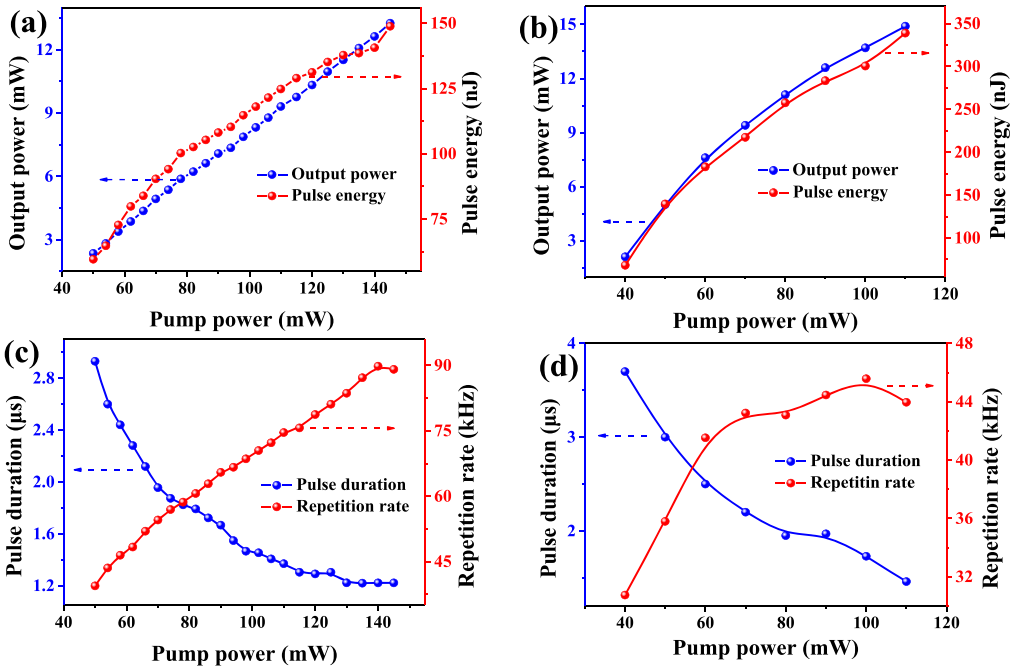

Figure 5. The Q-switching output power and pulse energy of (a) $Mo_{0.5}W_{0.5}S_2$-PVA film SA and (b) fiber-taper SA. The Q-switching pulse duration and repetition rate of (c) $Mo_{0.5}W_{0.5}S_2$-PVA film SA and (d) fiber-taper SA.

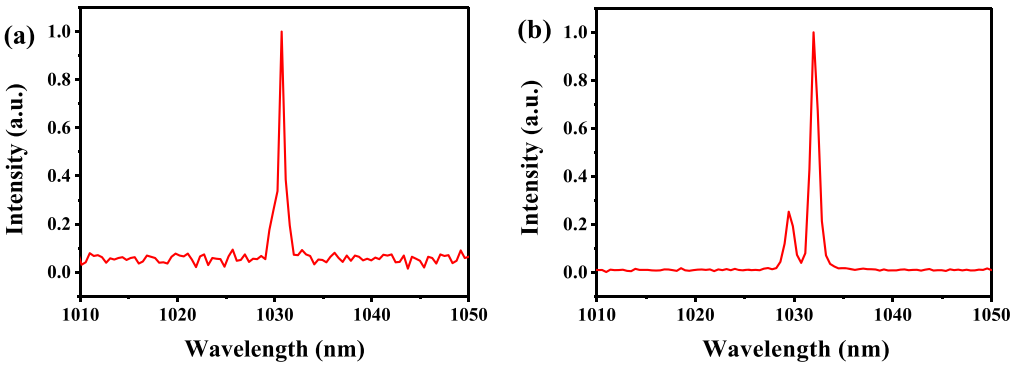

Figure 6. The output spectrum of the Q-switched YDF laser based on (a) $Mo_{0.5}W_{0.5}S_2$-PVA film SA and (b) $Mo_{0.5}W_{0.5}S_2$ fiber-taper SA at the pump power of 110 mW.

Table 2. Typical Q-switched results on TMDs of YDF lasers in recent reports.

SA	Min. pulse duration/ μs	Max. pulse energy/ nJ	Repetition rate/kHz	References
MoS_2	2.88	126	65.3–89.0	[34]
MoS_2	5.8	32.6	6.4–28.9	[35]
WS_2	1.0	56.5	36.78–81.75	[36]
WS_2	1.65	28.8	60.2–97.0	[37]
$MoSe_2$	2.8	116	60–74.9	[16]
$Mo_{0.5}W_{0.5}S_2$	1.22	148.8	39.44–89.09	this work
$Mo_{0.5}W_{0.5}S_2$	1.46	339	30.57–44.58	this work

in figure 4(e) in a wide span of 500 kHz. We only observed the fundamental and the harmonic frequencies in the RF output spectrum (the inset of figure 4(e)), which further confirmed the stability of the Q-switching operation. The RF spectrum analyzer (Rigol DSA815) has a minimum resolution bandwidth of 100 Hz. The signal to noise ratio is 39 dB with the film SA.

As the nonlinear transmittance is influenced by the laser intensity, in this case, when the pump power is changed, the output laser pulse should also change. Figures 5(a) and (b) show the output power and the pulse energy of two type of SAs increase almost linearly with the increasing of the pump power. The largest output powers and pulse energies obtained are 13.26 mW and 148.8 nJ for the film SA and 14.9 mW and 339 nJ for the fiber-taper SA. The results shows that Q-switched fiber laser with the taper-fiber $Mo_{0.5}W_{0.5}S_2$ SA has a higher slope efficiency and higher single pulse energy. This difference is due to the different way in which the laser pulses interact with the film SA. The direct interaction method for the film SA will introduce large non-saturation loss and increase the loss in the cavity, result in less efficient. Meanwhile, the direct interaction method makes the SA very easy

to saturate under low laser intensity, therefore the pulse energy with film SA is relatively low. However, the indirect interaction method for tapered fiber SA can avoid these issues. We think that the taper-fiber SA may have lower non-saturable loss and larger saturation intensity.

The pulse duration and repetition rate are another two important parameters for the Q-switched fiber lasers. As shown in figures 5(c) and (d), the minimum pulse durations and maximum repetition rate of the Q-switched fiber laser based on film SA and fiber-taper SA are 1.22 μs and 1.46 μs, 89.09 kHz and 45.58 kHz respectively. As shown in figure 5(c), in the beginning, with the pump power increasing, the the reduction of the pulse width is obvious and the output pulse is more and more stable due to the saturation of the SA. Under higher incident power, the change of the pulse width slow down. However, for the Q-switching with film SA, when the pump power exceeds 145 mW, the Q-switching operation disappears, the Q-switched pulse can be obtained again by reducing of the pump power. This phenomenon suggests that the disappearance of the laser pulse is not due to the damage of the SA but for the oversaturation [33, 36]. Figure 6(a) shows the optical spectrum of the laser output based on $Mo_{0.5}W_{0.5}S_2$-PVA film SA, whereas the center-wavelength is 1030.70 nm. As shown in figure 5(d), the pulse duration of the Q-switched fiber laser based on fiber-taper $Mo_{0.5}W_{0.5}S_2$ linearly decreases with the pump power. The minimum pulse duration is 1.46 μs at the pump power of 110 mW. Taking into account the interaction of the laser pulse and the SA is weak, the short pulse duration benefits from the long interaction length of the fiber-taper SA. The slight fluctuations of the repetition rate could be related to the competition between different wavelengths. When the pump increases to 80 mW, a new wavelength appears on the left side of the spectrum as shown in figure 6(b). The new wavelength competes with the existed Q-switching laser and partially bleaches the SA, which results in the fluctuation of the repetition rate.

Table 2 shows the typical Q-switched result on TMDs of YDF lasers in recent reports [16, 34–37]. It is seen that the $Mo_{0.5}W_{0.5}S_2$ SA shows excellent performance in both pulse width and single pulse energy. The $Mo_{0.5}W_{0.5}S_2$ SA has a narrower pulse width as comparable with MoS_2 and WS_2 SA and is superior on the single pulse energy. To further improve the Q-switching performance or even obtain mode-locking operation, one could optimize the fabrication method of the $Mo_{0.5}W_{0.5}S_2$, reduce the cavity loss and increases the strength of the interaction between the SA and the laser pulses.

4. Conclusions

In conclusion, the Q-switched operations based on $Mo_{0.5}W_{0.5}S_2$-PVA film and fiber-taper $Mo_{0.5}W_{0.5}S_2$ SA have been demonstrated in all-fiber YDF lasers. The modulation depth and saturable intensity of the film SA are 5.63% and 6.82 MW cm^{-2}. Based on the $Mo_{0.5}W_{0.5}S_2$-PVA film SA, Q-switched pulses with pulse energy of 148.8 nJ is realized. The minimum pulse duration is 1.22 μs. Higher pulse energy of 339 nJ and pulse width of 1.46 μs are also obtained with the fiber-taper $Mo_{0.5}W_{0.5}S_2$ SA. The results indicate the excellent performance of the $Mo_{0.5}W_{0.5}S_2$ SA for the pulse laser applications. To our best knowledge, this is the first report on the Q-switched YDFL based on $Mo_{0.5}W_{0.5}S_2$ SA. We believe that it will have greater potential applications in the nonlinear optics and ultrafast photonics. Moreover, the nonlinear optical properties of other $Mo_{1-x}W_xS_2$ alloys with different atomic proportions also require investigating in the next work.

Acknowledgments

This work is partly supported by National Natural Science Foundation of China (61675158).

ORCID iDs

Junli Wang https://orcid.org/0000-0003-1718-5024

References

[1] Keller U 2003 Recent developments in compact ultrafast lasers *Nature* **424** 831–8
[2] Paschotta R, Häring R, Gini E, Melchior H, Keller U, Offerhaus H L and Richardson D J 1999 Passively Q-switched 0.1 mJ fiber laser system at 1.53 μm *Opt. Lett.* **24** 388–90
[3] Skorczakowski M *et al* 2010 Mid-infrared Q-switched Er:YAG laser for medical applications *Laser Phys. Lett.* **7** 498–504
[4] Ren J, Wang S X, Cheng Z C, Yu H H, Zhang H J, Chen Y X, Mei L M and Wang P 2015 Passively Q-switched nanosecond erbium-doped fiber laser with MoS_2 saturable absorber *Opt. Express* **23** 5607–13
[5] Gao C, Zhao W, Wang Y S, Zhu S L, Chen G F and Wang Y G 2007 Passive Q-switched fiber laser with SESAM in ytterbium-doped double clad fiber *Proc. SPIE* **6279** 62794G–G6
[6] Yu Z H, Song Y R, Tian C C, Li J, Zhang X and Wang Y G 2012 Q-switched Yb-doped double cladding fiber laser with single wall carbon nanotube saturable absorber *Photonics Asia* **8551** 855115
[7] Woodward R I and Kelleher E J 2015 2D saturable absorber for fiber lasers *Appl. Sci.* **5** 1440–56
[8] Sobon G 2015 Mode-locking of fiber lasers using novel two-dimensional nanomaterials: graphene and topological insulators [Invited] *Photon. Res.* **3** A56–63
[9] Wu K *et al* 2018 High-performance mode-locked and Q-switched fiber lasers based on novel 2D materials of topological insulators, transition metal dichalcogenides and black phosphorus: review and perspective (invited) *Opt. Commun.* **406** 214–29
[10] Radisavljevic B, Radenovic A, Brivio J, Giacometti V and Kis A 2011 Single-layer MoS_2 transistors *Nat. Nanotechnol.* **6** 147–50
[11] Yu S L, Wu X Q, Wang Y P, Guo X and Tong L M 2017 2D materials for optical modulation: challenges and opportunities *Adv. Mater.* **29** 201606128
[12] Luo Z Q *et al* 2015 Two-dimensional materials saturable absorbers: towards compact visible-wavelength all-fiber pulsed lasers *Nanoscale* **8** 1066–72

[13] Xia F N 2014 Two-dimensional material nanophotonics *Nat. Photon.* **8** 899–907

[14] Wei R F, Zhang H, Hu Z L, Qiao T, He X, Guo Q B, Tian X L, Chen Z and Qiu J R 2016 Ultra-broadband nonlinear saturable absorption of high-yield MoS_2 nanosheets *Nanotechnology* **27** 305203

[15] Huang Y Z, Luo Z Q, Li Y Y, Zhong M, Xu B, Che K, Xu H Y, Cai Z P, Peng J and Weng J 2014 Widely-tunable, passively Q-switched erbium-doped fiber laser with few-layer MoS_2 saturable absorber *Opt. Express* **22** 25258–66

[16] Woodward R I, Howe R C, Runcorn T H, Hu G, Torrisi F, Kelleher E J and Hasan T 2015 Wideband saturable absorption in few-layer molybdenum diselenide ($MoSe_2$) for Q-switching Yb-, Er- and Tm-doped fiber lasers *Opt. Express* **23** 20051–61

[17] Ahmad H, Ruslan N E, Ismail M A, Reduan S A, Lee C S, Sathiyan S, Sivabalan S and Harun S W 2016 Passively Q-switched erbium-doped fiber laser at C-band region based on WS_2 saturable absorber *Appl. Opt.* **55** 1001–5

[18] Chen B H, Zhang X Y, Guo C S, Wu K, Chen J P and Wang J 2016 Tungsten diselenide Q-switched erbium-doped fiber laser *Opt. Eng.* **55** 081306

[19] Zeng Q S, Wang H, Fu W, Gong Y J, Zhou W, Ajayan P M, Lou J and Liu Z 2015 Band engineering for novel two-dimensional atomic layers *Small* **11** 1868

[20] Nasruddin M N, Sigiro M and Fahmi M R 2015 Raman scattering characterization of $Mo_xW_{1-x}S_2$ layered mixed crystals *Applied Mechanics & Materials* **754-755** 595–601

[21] Qiao X F, Li X L, Zhang X, Shi W, Wu J B, Chen T and Tan P H 2015 Substrate-free layer-number identification of two-dimensional materials: a case of $Mo_{0.5}W_{0.5}S_2$ alloy *Appl. Phys. Lett.* **106** 666

[22] Xie L M 2015 Two-dimensional transition metal dichalcogenide alloys: preparation, characterization and applications *Nanoscale* **7** 18392–401

[23] Wang X S, Xie L M and Zhang J 2015 Preparation, structure and properties of two-dimensional semiconductor alloys *Acta Chim. Sin.* **73** 886–94

[24] Chen Y F, Xi J Y, Dumcenco D O, Liu Z, Suenaga K, Wang D, Shuai Z G, Huang Y S and Xie L M 2013 Tunable band gap photoluminescence from atomically thin transition-metal dichalcogenide alloys *ACS Nano* **7** 4610

[25] Bikorimana S, Lama P, Walser A, Dorsinville R, Anghel S, Mitioglu A, Micu A and Kulyuk L 2016 Nonlinear optical responses in two-dimensional transition metal dichalcogenide multilayer: WS_2, WSe_2, MoS_2 and $Mo_{0.5}W_{0.5}S_2$ *Opt. Express* **24** 20685–95

[26] Li J P, Mo G L, Bai Y H and Bao A 2015 Microwave-assistant hydrothermal synthesis and luminescence of $NaEu(MoO_4)_2$:Sm^{3+} powders *Mater. Sci: Mater. Electron.* **26** 7390–6

[27] Liu W J, Pang L H, Han H N, Bi K, Lei M and Wei Z Y 2017 Tungsten disulphide for ultrashort pulse generation in all-fiber lasers *Nanoscale* **9** 5806–11

[28] Chen B H, Zhang X Y, Wu K, Wang H, Wang J and Chen J P 2015 Q-switched fiber laser based on transition metal dichalcogenides MoS_2, $MoSe_2$, WS_2, and WSe_2 *Opt. Express* **23** 26723–37

[29] Zang Z G and Zhang Y J 2012 Analysis of optical switching in a Yb^{3+}-doped fiber Bragg grating by using self-phase modulation and cross-phase modulation *Appl. Opt.* **51** 3424–30

[30] Zang Z G and Zhang Y J 2012 Low-switching power (<45 mW) optical bistability based on optical nonlinearity of ytterbium-doped fiber with a fiber Bragg grating pair *J. Mod. Opt.* **59** 161–5

[31] Paschotta R, Nilsson J, Tropper A C and Hanna D C 2001 Ytterbium-doped fiber amplifiers *IEEE J. Quantum Electron.* **33** 1049–56

[32] Furusawa K, Malinowski A, Price J, Monro T, Sahu J, Nilsson J and Richardson D 2001 Cladding pumped Ytterbium-doped fiber laser with holey inner and outer cladding *Opt. Express* **9** 714–20

[33] Li H P, Xia H D, Lan C Y, Li C, Zhang X X, Li J F and Liu Y 2015 Passively Q-switched erbium-doped fiber laser based on few-layer MoS_2 saturable absorber *IEEE Photonics Technol. Lett.* **27** 69–72

[34] Woodward R I, Kelleher E J, Howe R C T, Hu G, Torrisi F, Hasan T, Popov S V and Taylor J R 2014 Tunable Q-switched fiber laser based on saturable edge-state absorption in few-layer molybdenum disulfide (MoS_2) *Opt. Express* **22** 31113–22

[35] Luo Z Q, Huang Y Z, Zhong M, Li Y Y, Wu J Y, Xu B, Xu H Y, Cai Z P, Peng J and Weng J 2014 1-, 1.5-, and 2 μm fiber lasers Q-switched by a broadband few-layer MoS_2 saturable absorber *J. Lightwave Technol.* **32** 4077–84

[36] Wang J L, Li S, Xing Y P, Chen L, Wei Z Y and Wang Y G 2017 A high-energy passively Q-switched Yb-doped fiber laser based on WS_2 and Bi_2Te_3 saturable absorbers *J. Opt.* **19** 095506

[37] Lin J, Hu Y Y, Chen C J, Gu C and Xu L X 2015 Wavelength-tunable Yb-doped passively Q-switching fiber laser based on WS_2 saturable absorber *Opt. Express* **23** 29059–64